OPEN ACCESS
OPUS AUGSBURG

Universität Augsburg
Universitätsbibliothek

Investigating superconductivity with Electron Paramagnetic Resonance (EPR) spectrometer

D. Shaltiel, Hans-Albrecht Krug von Nidda, B. Ya. Shapiro, Alois Loidl, T. Tamegai, T. Kurz, B. Bogoslavsky, B. Rosenstein, I. Shapiro

Angaben zur Veröffentlichung / Publication details:

Shaltiel, D., Hans-Albrecht Krug von Nidda, B. Ya. Shapiro, Alois Loidl, T. Tamegai, T. Kurz, B. Bogoslavsky, B. Rosenstein, and I. Shapiro. 2012. "Investigating superconductivity with Electron Paramagnetic Resonance (EPR) spectrometer." In *Superconductors - Properties, Technology, and Applications*, edited by Yury Grigorashvili, 63–82. London: InTech. https://doi.org/10.5772/38175.

Nutzungsbedingungen / Terms of use: **CC BY 3.0**

Dieses Dokument wird unter folgenden Bedingungen zur Verfügung gestellt: / This document is made available under these conditions:
CC-BY 3.0: Creative Commons - Namensnennung
Weitere Informationen finden Sie unter: / For more information see:
https://creativecommons.org/licenses/by/3.0/de/deed.de

4

Investigating Superconductivity with Electron Paramagnetic Resonance (EPR) Spectrometer

D. Shaltiel et al*
The Hebrew University of Jerusalem
Israel

1. Introduction

Shortly after the discovery of high T_c superconductors there was an influx of publications where EPR technique was used to investigate their properties (Srinivasu et al., 2001). As no substantial information was obtained it was soon almost abandoned. The fact that EPR technique provided a large number of experimental data in the superconducting regime, without significantly contributing to the deeper understanding of high T_c superconductors was puzzling. Meanwhile, our continuous effort to further investigate superconductivity using EPR technique yielded important experimental and theoretical results related to properties of high T_c superconductors. Furthermore, some of these results are unique as they were not obtained with conventional experimental techniques.

The work shows that an electron paramagnetic resonance spectrometer is a powerful tool to investigate properties of superconductors. As superconducting systems are not conventional paramagnetic substances, the EPR signals do not originate from the usual resonant absorption, namely magnetic dipolar transitions between spin levels. Thus, it is essential in analyzing the experimental results, to explore the mechanism that induces the EPR signals. Indeed, by detailed experimental and theoretical studies of the EPR spectra of different high T_c superconductors, it has been possible to apprehend the mechanism that induces the observed microwave absorption. Based on these results, new unknown properties of superconductors were obtained. As the EPR spectrometer is the central experimental tool in the present work, we start by describing the EPR spectrometer in details, to facilitate the reader understanding its various functions. This step is necessary, as it turned out that among experts in superconductivity many are not familiar with the elements of the EPR spectrometer, how and what it measures. We will then continue by presenting experimental

*H.A. Krug von Nidda[2], B.Ya. Shapiro[3], A. Loidl[2], T. Tamegai[4], T. Kurz[2], B. Bogoslavsky[1], B. Rosenstein[5,6] and I. Shapiro[3]
[1]*The Hebrew University of Jerusalem, Israel*
[2]*Experimental Physics V, Center for Electronic Correlations and Magnetism, University of Augsburg, Augsburg, Germany*
[3]*Bar-Ilan University, Ramat-Gan, Israel*
[4]*The University of Tokyo, Hongo, Japan*
[5]*National Chiao Tung University, Department of Electrophysics, Hsinchu, Taiwan, R.O.C.*
[6]*Ariel University Center, Israel*

results obtained in high T_c superconductors subjected to various factors such as DC and AC magnetic fields, temperature, sample orientation and to different sample treatments such as zero-field-cooling or field-cooling. This overview will allow a systematic classification of the measurements and will provide the theoretical background (Shaltiel et al., 2008) necessary to analyze these experiments and to understand the inherent physics. The presentation is based on publications by the authors over a period from just after the discovery of high T_c superconductors to date.

2. Experimental

An EPR spectrometer, Fig. 1**,** consists of a microwave source that feeds a cavity where a sample is installed. The sample is exposed to three magnetic fields; a DC field, H_{DC}, a collinear low frequency AC field, h_{AC}, and a transverse microwave field, H_{rf}. The microwave and the AC frequencies used in the present investigation were 9.3 GHz and 100 kHz, respectively. At zero DC field the coupling of the waveguide to the cavity is adjusted critically in such a way that the reflection from the cavity is zero. Regarding a usual EPR experiment on a paramagnetic sample, the variation of the DC field results in a detuning from the critical adjustment on passing the resonance condition for magnetic dipolar transitions between the Zeeman levels ($\nu=\gamma H_{DC}$, with microwave frequency ν and gyromagnetic ratio γ) and in turn yields microwave reflection from the cavity. The reflected microwave power is rectified by a detector, i.e. a microwave diode, yielding a signal proportional to the absolute value of the reflected power P at H_{DC} and modulated by the AC frequency (note that $h_{AC}<<H_{DC}$). This signal is further fed into a lock-in-detector **(LID)** which samples the signal by convolution with a periodic signal of the same AC frequency over a large number of AC periods, thus yielding amplitude and phase while suppressing statistical noise. Provided that the width of the resonance absorption dependent on H_{DC} is larger than the amplitude of the AC modulation field h_{AC}, the LID output submits a signal proportional to the field derivative of the paramagnetic resonance signal dP/dH.

An accepted assumption in analyzing experimental results obtained by an EPR spectrometer is that the role of the AC field is to introduce variations in the magnitude of the DC magnetic field; the AC field is usually referred to as the modulating magnetic field. However, as will be shown below, the AC field does not just result in a modulation of the microwave signal dependent of the modulated static field like in a usual EPR experiment, but in superconductors it may also induce an additional mechanism of microwave power dissipation.

Therefore, one should be perceptive to the different dissipation process, when analyzing the EPR results in the superconducting phase. Here it is important to note that a complication in the measuring process has been observed. It is related to variations in the signal phase that may develop through the measuring process. The reference AC phase of the LID is adjusted for usual EPR measurements to yield the optimum paramagnetic resonance signal. However in case of the microwave dissipation observed in anisotropic superconductors this adjustment turns out to be not appropriate. Variations in the signal phase were observed when varying the magnitude of the variables involved such as DC magnetic field, temperature, sample orientation and others. This effect necessitates a procedure where the lock-in detector phase has to be adjusted, throughout the measuring process, to be in-phase with the AC phase. To overcome this problem, conducted during the measuring process, the

measurements were performed in steps of the variables involved, and at each step the lock-in detector phase had to be adjusted accordingly. This procedure results in an extremely cumbersome measurement, where the possibilities offered by the modern EPR Bruker spectrometer ELEXSYS E500 are extremely useful. A feature of this spectrometer is its possibility to measure the signal intensity in steps of two variables. It allows obtaining the measured signal intensity at each step, where the lock-in phase is varied from zero to 180^0. Repeating the measurement, by changing, in steps, the magnitude of the variable involved (such as magnetic field, temperature, angle of the oriented crystal) gives the measured signal intensity as function of the variable at the full 180^0 range of the lock-in phase. Then the measurements were analyzed using a proper computer program. It allowed obtaining two curves, the measured signal amplitude, and the corresponding signal phase, as a function of the variable involved such as: DC magnetic field, AC magnetic field, sample orientation angle and temperature. Thus, the actual "calculated" signal was derived from the measured signal amplitude and its corresponding signal phase (see below).

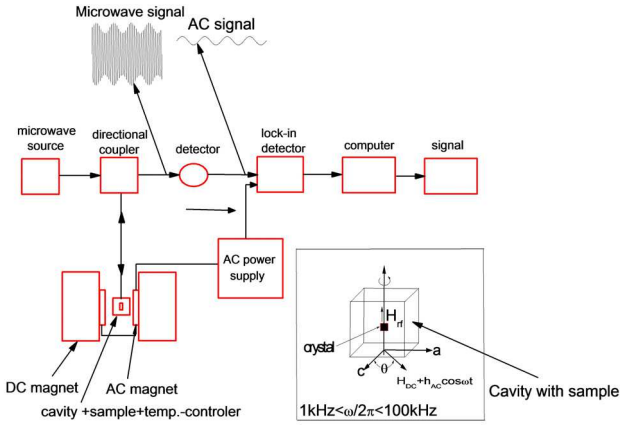

Fig. 1. Block diagram of the EPR spectrometer.

Fig. 2 presents such a result, for a $Bi_2Sr_2CaCu_2O_{8+\delta}$ (Bi2212) single crystal, Zero Field Cooled **(ZFC)** to 4K with the DC magnetic field applied parallel to the a-b plane. The upper curve shows the measured signal amplitude, and the lower curve shows its corresponding signal phase (with respect to the lock-in AC phase) as function of DC magnetic field. The measured signal amplitude exhibits two maxima followed by an exponential decay towards zero at high fields. The signal phase is close to zero at low fields and drops steeply towards -180^0 at high fields. It indicates that the signal is in phase and out of phase with the AC field at low and high fields, respectively. The details of the phase shift, i.e. deviations (±20°) from 0° at low fields and from 180° at high fields have not been investigated so far and need further attention. As the allover phase shift from low to high fields is evidently less than 180° it cannot be explained just by a constant shift of the calibration.

Fig. 3 presents EPR results similar to those shown in Fig. 2, for temperatures, 80K, 30K and 4K. It indicates that the measured signal amplitude and signal phase have similar functional behavior as in Fig. 2. It implies that the EPR responses as function of field are similar in the temperature range from T_c down to 4K.

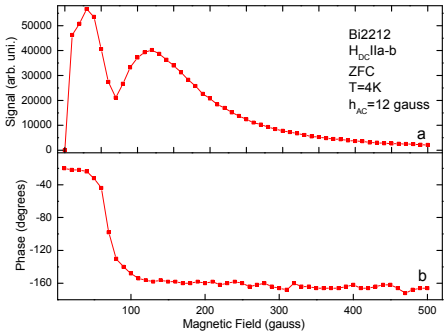

Fig. 2. AC induced microwave dissipation signal amplitude (a) with the corresponding phase value (b) of a Bi2212 single crystal, ZFC to 4K, as function of DC magnetic field aligned parallel to the a-b plane.

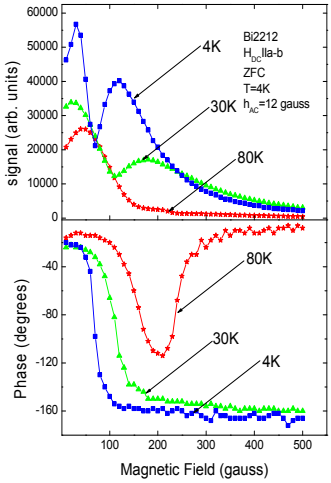

Fig. 3. AC induced microwave dissipation signal amplitudes with their corresponding phase values, of the same Bi2212 single crystal shown in Fig. 2, ZFC to 80K, 30K, and 4K, as function of DC magnetic field aligned parallel to the a-b plane.

Understanding the mechanism that induces the signal, the origin of the spectra, and its corresponding signal-phase as function of field, is an important key in studying superconducting properties with the EPR spectrometer.

Fig. 4 shows the actual calculated signal as function of field in Bi2212, derived by multiplying the measured signal amplitude of Fig. 2 with the cosine of its phase. It shows a sharp increase in the intensity at very low magnetic field followed by a steep decrease with change of sign to negative values and a final increase that asymptotically tends to zero. The theoretical considerations presented in (Shaltiel et al., 2008) showed that this corresponds to the field derivative of the dissipated microwave power due to shaking of JV away from the zero crossing, but is subject to strong nonlinearities close to the zero crossing.

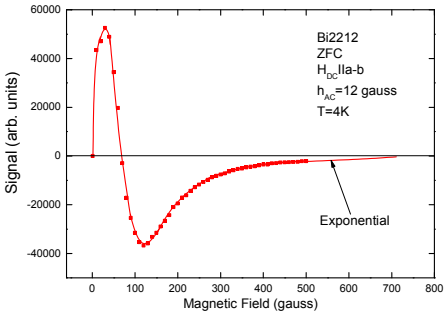

Fig. 4. Actual calculated signal in the Bi2212 crystal as function of field parallel to the conduction plane at 4K, derived by multiplying the measured signal amplitude with the cosine of its corresponding phase using the values shown in Fig. 2.

Fig. 5 presents the measured signal amplitude and the corresponding signal phase as function of magnetic field applied parallel to the a-b plane for a $Bi_2Sr_2Ca_2Cu_3O_{10+x}$ (Bi2223) single crystal ZFC to 4K. It shows a response similar to the observed signal in Fig. 2 for Bi2212. As both Bi2212 and Bi2223 are high-anisotropy superconductors, we deduce that a high anisotropy is a necessary condition to observe similar results in the high-T_c superconductors. This conjecture is also confirmed by our measurements in the high-T_c, low-anisotropy YBCO ($YBa_2Cu_3O_{7-\delta}$) superconductor: no significant EPR signal was observed in optimally dopes YBCO, when the DC magnetic field is applied either parallel or perpendicular to the a-b plane, while sizable signals appeared for overdoped, i.e. more anisotropic YBCO with the magnetic field applied within the a-b plane. These recent results are intended to be published elsewhere. Fig. 6 presents the actual calculated signal as a function of field in Bi2223 derived from the measured signal amplitude and from its corresponding signal phase of Fig. 5. It shows a similar DC-field dependence like that observed in Fig. 4 for Bi2212. It confirms again the earlier conclusion that high-anisotropy is a necessary condition for obtaining a similar behavior in different superconductors.

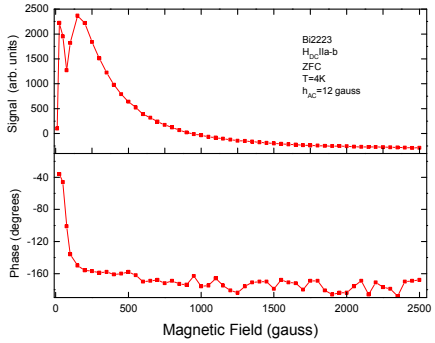

Fig. 5. AC induced microwave dissipation signal amplitude with the corresponding phase value of a Bi2223 single crystal, ZFC to 4K, as function of magnetic field aligned parallel to the a-b plane. The temperature behavior of the signals in Bi2223 is similar to that observed in Bi2212.

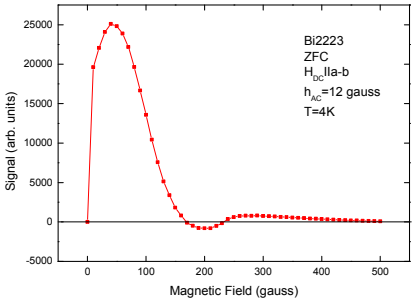

Fig. 6. Actual calculated signal in the Bi2223 crystal as function of field parallel to the conduction plane at 4K, derived by multiplying the measured signal amplitude with the cosine of its corresponding phase using the values shown in Fig. 3.

The experimental results presented in Figs. 2-6 show the EPR signal as a function of DC magnetic field using a constant AC field. An additional picture is obtained by interchanging the roles of the variables, namely the DC field is kept constant and the EPR signal is measured as function of AC field. Such a result is illustrated in Fig. 7**;** it shows the signal amplitude and signal phase as function of AC magnetic field for a Bi2212 crystal. The measurements were performed by zero-field cooling the crystal down to 30K, followed by applying a DC field of 20 gauss or 150 gauss, prior to sweeping the AC field. The figure shows striking differences in the signal amplitude and in the signal phase as function of AC field when either of the two DC fields is applied. The 20 gauss signal amplitude increases strongly and linearly with increasing AC field. In contrast, the 150 gauss signal amplitude - after a slight increase - remains low and constant. At low AC field the two signals are out of phase with respect to the AC phase. At high AC field the signals are in phase and out of phase respectively when either the low or the high DC field are applied.

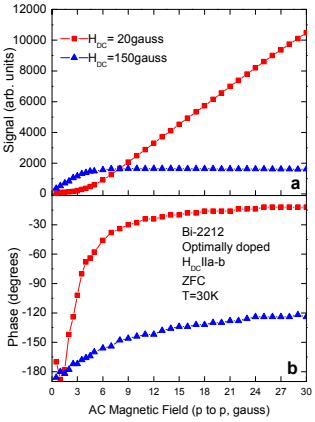

Fig. 7. Signal amplitude (a) and signal phase (b) in Bi2212 vs. AC magnetic field, obtained by zero-field cooling the crystal to 30K, followed by applying a DC field of 20 gauss or 150 gauss prior to sweeping the AC field.

Similar results are observed for a Bi2223 superconductor as shown in **Fig. 8**. They were obtained by zero-field cooling the crystal down to 30K, followed by application of a DC field of 30 gauss, 500 gauss or 5000 gauss prior to sweeping the AC field. Here again, as with the Bi2212 crystal, the Bi2223 signal amplitude, obtained when the low magnetic field of 30 gauss was applied, increases strongly and linearly with increasing AC field, whilst the signal amplitude observed, when 500 gauss was applied, is low and remains constant with increasing AC field. The signal obtained, when the much stronger 5000 gauss cooling field was applied, shows negligibly small signal amplitude for all AC field values. It confirms the previous conclusion regarding the similarity of EPR response in different high anisotropy superconductors.

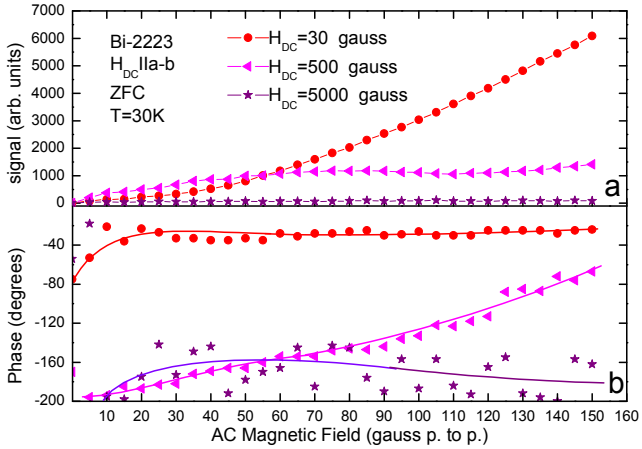

Fig. 8. Signal amplitude (a) and signal phase (b) in Bi2223 vs. AC magnetic field, obtained by zero-field cooling the crystal to 30K, followed by applying a DC field of 30 gauss or 500 gauss or 5000 gauss prior to sweeping the AC field.

3. Understanding the physics of the AC-field-induced signals

Fig. 9 presents an extremely important result vital to understand the physics, and to comprehend the mechanism of the AC field induced microwave dissipation results in the highly anisotropic superconductors. The figure shows an unexpected effect where the signal intensity as function of temperature in the high anisotropy Bi2212 crystal for the DC magnetic field aligned parallel to the c-axis is zero from T_c to 4K, whilst at DC magnetic field parallel to the a-b plane, the signal intensity increases sharply already just below T_c and continues to increase sharply towards lower temperatures. The small signal observed close to T_c in Fig. 9 for the DC magnetic field applied parallel to the c-axis results from the thermally activated flux flow resistivity (FFR) (Shaltiel et al., 2001). (See Fig. 6 of Shaltiel et al., 2001)

A reasonable conclusion to the extreme difference in the superconducting response under the parallel and the perpendicular DC magnetic field, is derived from Fig. 10. It shows that, when a magnetic field is parallel to the a-b plane, only Josephson vortices (JV) are formed and, while applying a magnetic field parallel to the c-axis, only Abricosov vortices, i.e.

pancake vortices (PV), are formed. This indicates that the AC magnetic field induces microwave dissipation, when interacting with JV, but none when interacting with PV.

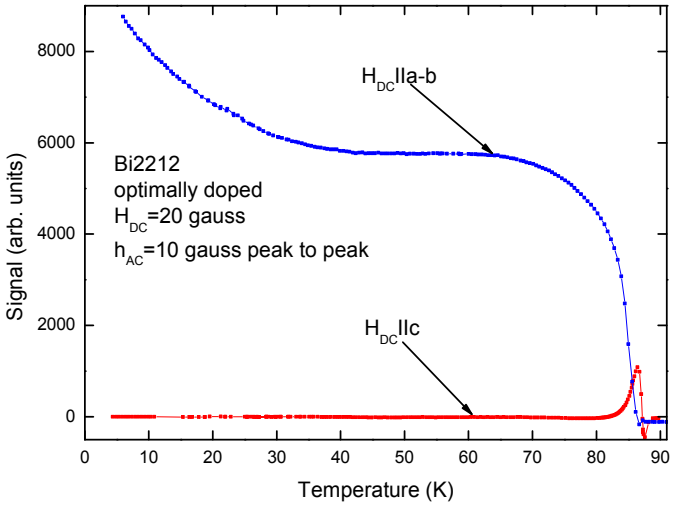

Fig. 9. Signal amplitude as function of temperature in the high anisotropy Bi2212 crystal for DC magnetic field aligned parallel to the a-b plane or to the c-axis. Note the large different response for the two orientations. The small signal observed close to Tc for magnetic field parallel to the c-axis results from thermally activated flux flow resistivity.

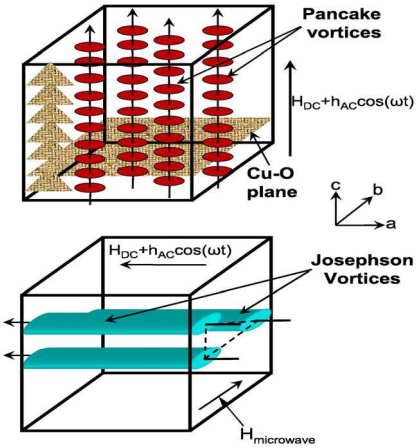

Vortex structure for magnetic field parallel or perpendicular to the a-b plane

Fig. 10. The figure shows that applying a magnetic field parallel to the a-b plane forms only JV, whilst, applying a magnetic field parallel to the c-axis forms only PV.

This conclusion is corroborated by the fact that microwave dissipation results similar to those shown in Fig. 7, were observed also in Bi2223 which like in Bi2212 forms JV and PV for the magnetic field applied parallel and perpendicular to the a-b plane, respectively. Moreover, we recall that, unlike in Bi2212 or in Bi2223, no significant microwave dissipation was observed in optimally doped $YBa_2Cu_3O_{7-\delta}$ for any direction of the external DC magnetic field besides the signal at T_c from the thermally activated flux flow resistivity. As only PV are formed in optimally doped $YBa_2Cu_3O_{7-\delta}$ for all magnetic field orientations, this again confirms the conclusion that no microwave dissipation is induced by the AC magnetic field, when interacting with PV.

A mechanism that explains the induced microwave dissipation by the AC field, when interacting with JV, is derived from soliton propagation in Josephson transition lines observed in itinerant Josephson junction (IJJ) mesas (Hechtfischer et al., 1997)**.** Such a mesa is given in Fig. 11[1] : A DC bias current applied parallel to the a-b plane induces a Lorentz force on the JV **(fluxons)** that reside between the conduction layers of the superconductor. Extremely high JV velocities, that may reach the speed of light, are obtained when the DC current is applied (Ustinov, 1998). The JV motion induces electromagnetic oscillations and, when interacting with the microwave field, microwave dissipation may result.

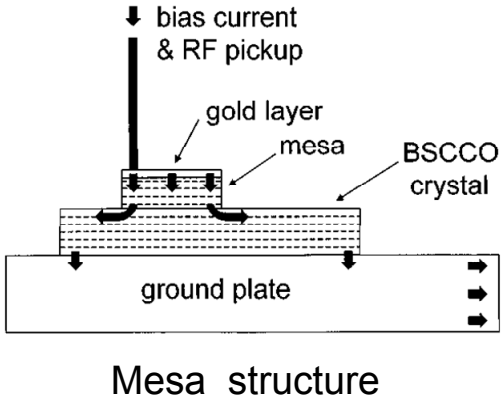

Fig. 11. Mesa structure of a BSCCO crystal. The bias current applies a Lorentz force on the JV that are present between the conduction planes.

Fig. 12 shows that the AC magnetic field applied parallel to the a-b plane induces oscillating Eddy currents in the conduction plane in a Bi2212 compound. As with the current in IJJ mesas, the Eddy currents give rise to a Lorentz force on the JV whose oscillating intensity induces oscillating interaction with the microwave field that generates the EPR microwave losses. This explains why EPR signals are observed at H||a-b plane but none at H||c-axis, as JV are formed only when the magnetic field is parallel to the conduction plane and are not formed when the field is parallel to the c axis. A straight forward conclusion in this analysis is that EPR dissipation signals in high anisotropy superconductors are observed only due to the motion of

[1] Permission to publish this figure (taken from Hechtfischer et al., 1997) was granted by APS, that keeps its copyrights).

JV. Therefore JV pinning plays an essential role on the signal shape. As JV pinning depends on the variables such as temperature and sample orientation, the analysis of the signal as a function of the variables involved enables the microscopic study of JV pinning.

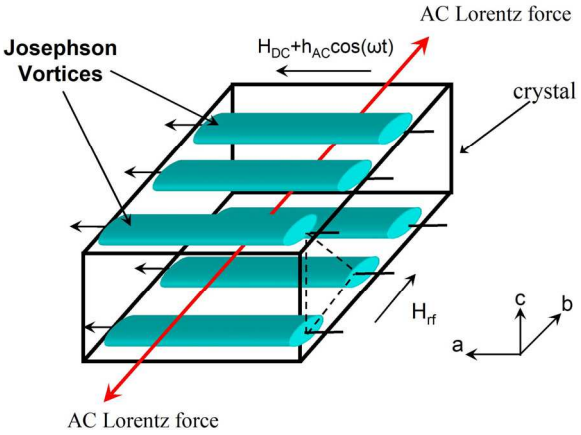

Fig. 12. Schematic picture that interprets the formation of AC-induced oscillating Eddy currents. The currents apply oscillating Lorentz forces on the Josephson vortices.

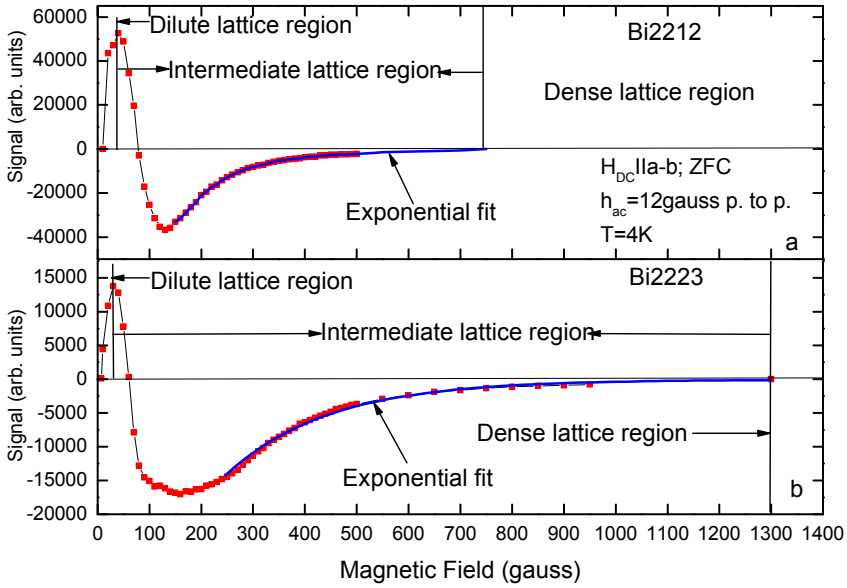

Fig. 13. Calculated signal in Bi2212 (a) and in Bi2223 (b) as a function of magnetic field parallel to the a-b plane at T=4K. It is obtained by multiplying the signal amplitude, with its corresponding phase. It shows formation of the dilute and dense region at low and high magnetic field respectively and an in-between intermediate region, in both compounds.

Fig. 13 presents the calculated signal of Bi2212 and Bi2223 as a function of magnetic field applied parallel to the a-b plane at T=4K**.** It is obtained by multiplying the measured signal amplitudes shown in Figs. 2 & 3, with their corresponding phase. It indicates the presence of three regions: A low field region, from zero to around 30 gauss, where the signal intensity increases almost linearly with field up to a maximum value; a high field region, where the signal intensity is zero; and an intermediate transition region. At low JV densities, the JV form the unpinned "dilute lattice region" due to negligible interaction between the JV. As the JV density increases linearly with the magnetic field, the Lorentz force on the JV induces a signal in the low-field region proportional to the DC field, as observed. At higher fields the inter JV interaction is strong and the JV form the "dense lattice region" where the JV are strongly pinned. The intensity of the AC field is not strong enough to induce motion of the JV in this region; therefore the signal intensity is zero. The inbetween intermediate region is characterized by a sharp decrease in the signal intensity and by an exponential decrease towards zero with increasing field. The field widths of the intermediate regions observed in Bi2212 and Bi2223 are different. This indicates a different distribution of the JV within the two compounds. The evolution of the JV system in the intermediate region has not been reported elsewhere.

4. Study of superconducting properties with EPR spectrometer

The theory which discusses the EPR experimental results was published earlier (Shaltiel et al., 2008). It shows that pinning of Josephson vortices effects strongly on their behavior. This section presents EPR results obtained in high anisotropic superconductors, which document the strength of this method in the investigation of the properties of Josephson vortices. It will also discuss the possibility to study small and nano-scale superconducting systems with EPR.

4.1 Interaction between Josephson vortices and Abricosov vortices

We have shown that the absence or presence of JV pinning is vital when investigating superconducting properties with the EPR technique. For example, the interaction of pancake vortices (PV), also known as Abrikosov vortices (AV), with JV induces pinning. Pinning of JV can be studied by varying the density of the Josephson vortices and Abricosov vortices in a controlled way and measuring the effect on the EPR signal. This can be achieved by tilting the orientation of a Bi2212 crystal, exposed to a given magnetic field H_{DC}, from magnetic field parallel to the a-b plane, where only JV are formed, towards the c-axis where only AV are formed. The density of the JV and PV as a function of the tilting angle, θ, of the magnetic field (θ being zero at magnetic field parallel to the a-b plane) varies as $\cos\theta$ and $\sin\theta$, respectively. Thus, the signal amplitude being proportional to the JV density should vary as $\cos\theta$, provided the JV remain unpinned. Deviation from $\cos\theta$ dependence would result from pinning of JV induced via the JV-AV interaction. This is demonstrated in **Fig. 14** for H_{DC}=20 gauss.

The figure shows that the signal amplitude decreases close to cos θ at θ values, 0^0 to 40^0. But at higher angles the signal amplitude decreases faster than cos θ. The increase in deviation indicates an increase in pinning above 40^0 due to the increase of the JV-AV interaction. As the pinning strength increases with angle, at angles below 40^0 the JV-AV interaction is not strong enough to induce an observable effect. The intensity of the interaction depends on H_i.

Increasing H_{DC} increases both JV and AV densities for all tilting angles. Therefore, the deviation from cos θ at higher H_{DC} should start at a lower tilting angle. This is observed in Fig. 15 for H_{DC} strengths of 20 gauss, 50 gauss, and 90 gauss where the deviation angle starts at 40^0, 20^0, and 5^0, respectively, indicating that the higher H_{DC} the lower the angle where the deviation starts. The systematic analysis of the signal amplitude as a function of the tilting angle for different H_{DC} values can be used to study the JV-AV interaction.

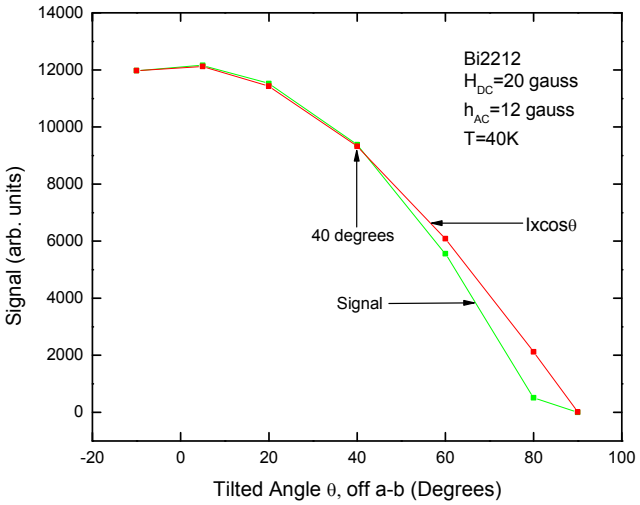

Fig. 14. Bi2212 signal amplitude as function of tilted angle θ in an applied field of 20 gauss.

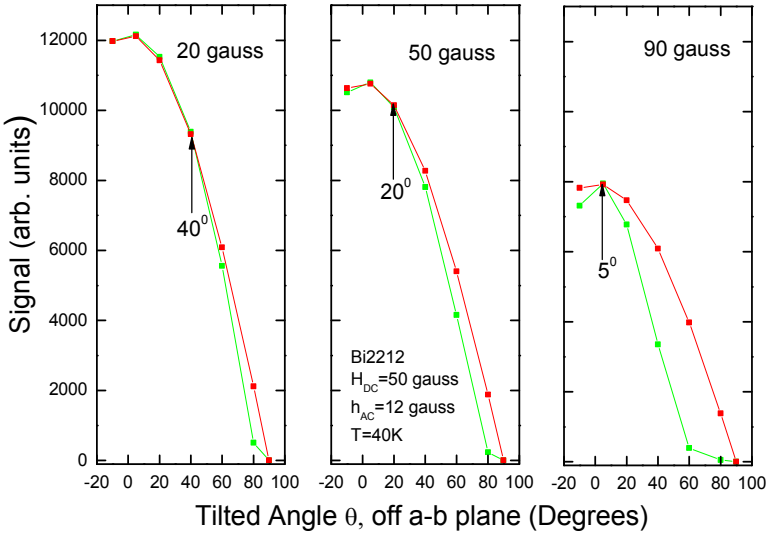

Fig. 15. Bi2212 signal ampltude as function of tilted angle θ in applied fields of 20 gauss, 50 gauss and 90 gauss.

4.2 Comparison of EPR signals, derived from either the field cooling or from the zero field cooling protocol using identical measurements

The maximum signal amplitude as function of temperature, derived from measurements of signal amplitude vs. magnetic field applied parallel to the a-b conduction planes in Bi2212, for zero field cooled (ZFC) protocol and for 500 gauss field cooled (FC) protocol is shown in Fig. 16. The maximum signal amplitudes were obtained from the corresponding maxima in the amplitude values similar to that shown in Fig 2. The figure shows that in both procedures, the maximum signal amplitudes have similar values from Tc down to 40K. Below 40K the maximum signal amplitude strongly increases for the ZFC measurement and sharply decreases for the FC measurement. The sharp decrease of the signal below 40K indicates that field cooling introduces pinning of JV. The increase of the ZFC signal indicates the absence, or only a very small pinning effect, of the JV below 40K.

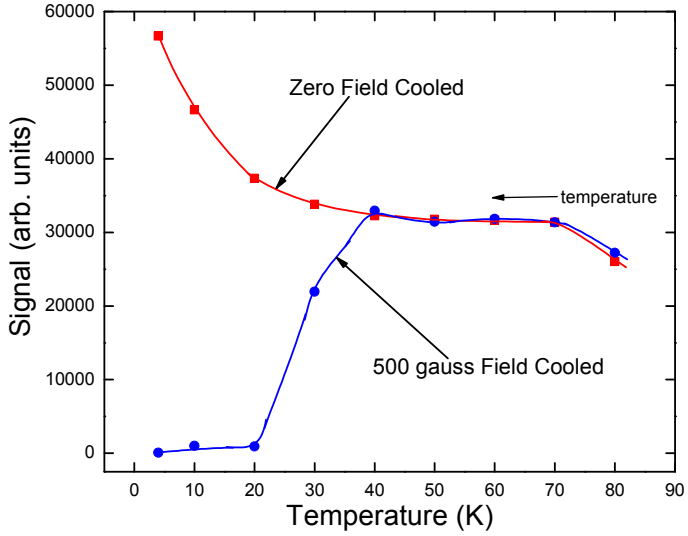

Fig. 16. Maximum signal amplitude as function of temperature in Bi2212 obtained when the sample is field cooled at either zero magnetic field or at 500 gauss magnetic field.

4.3 Memory effect

A memory signal is observed in the high anisotropy superconductors, Bi2212 and Bi2223. It is obtained by field cooling the superconductors in a magnetic field H_m, applied parallel to the conduction planes down to 4K, the lowest available temperature of the spectrometer. After setting the DC field to zero and then measuring the microwave dissipation on increasing DC field, a signal is observed slightly above H_m, indicating a **memory effect**. Memory signals are shown in Fig. 17 for Bi2212; with H_m values that range from 1500 gauss to 17000 gauss. (17000 gauss was the maximum available field with the operating spectrometer).

A detailed theoretical analysis of the memory effect was presented in an earlier publication (Shaltiel et al., 2010)**.** It indicates that by adiabatic field cooling from T_c to a low temperature, the JV explore the available phase space that nucleates into the deepest valley of the

landslide potential and are confined inside deep pinning landslide-potential minima in a quasi equilibrium glassy state. As the field is subsequently increased the fluxons are immobile and prevent penetration of new JV sites and cannot absorb microwave energy up to H_m. No signal was observed in this field region. When the magnetic field is increased above H_m new unpinned vortices start to penetrate.

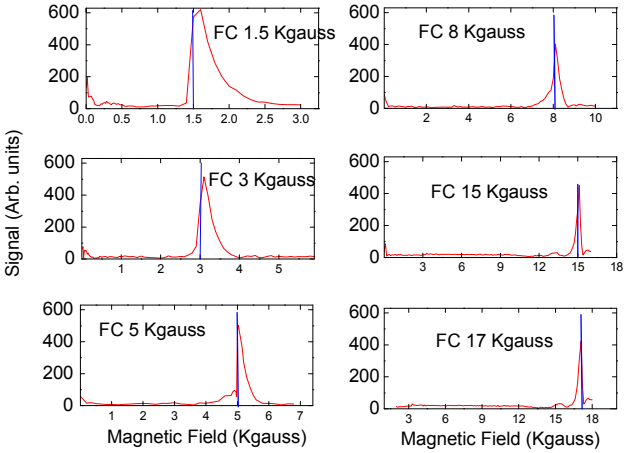

Fig. 17. Memory signal observed at magnetic fields, for H_m values 1.5 kgauss to 17 kgauss. Note that the memory signals appear at field values slightly above H_m.

Further analysis of the Bi2212 memory results presented in Fig. 17 demonstrates additional interesting properties. They indicate that the memory signals hold the following features, common to all H_m values: (a) the signals exhibit the same shape and retain similar intensities, and similar widths for all H_m values. (b) The field position H_{fp} of each memory signal occurs at a field slightly above H_m with similar H_{fp}-H_m value. (c) A narrow single-peak, small-intensity signal is observed at H=0 for all H_m values that decays strongly towards zero. d) In the field region from above H=0 to H=H_m, only a very weak signal is observed indicating the presence of a very small amount of unpinned Josephson vortices along this field region. Analyzing the memory features described in (a) to (d), implies the following additional properties: The signal shape of the memory signals described in (a) indicates similar features as those obtained in the signal shape of Fig. 2 presented earlier. The signal in Fig. 2 was obtained by zero field cooling the crystal (with the field oriented parallel to the a-b plane) followed by increasing the intensity of the magnetic field. In this process the AC field interacts with the JV that penetrate the crystal from H=0 and above, inducing the observed signal. The similarity between the signal shapes of Fig. 2 with the memory signals indicates that the same mechanism induces the memory signals in both cases. Thus as in Fig. 2, unpinned JV start to penetrate the crystal at magnetic fields above H_m, generating the memory effect. This conclusion is in agreement with the theoretical analysis given in reference (Shaltiel et al., 2010).

The analysis presented above in the field region where the memory signal is formed implies unexpected and intriguing consequences. It indicates that JV are present in the magnetic field region from zero to H_m. It predicts the formation of JV remanent magnetization in this

field region. To check this conjecture, the following procedure to measure the magnetization in a Bi2212 crystal was carried out. The magnetization was measured in a commercial SQUID (superconducting quantum interference device) magnetometer MPMS5 (Quantum Design) working in a temperature range from 1.8 < T < 400K and in magnetic fields up to 50 Kgauss. The Bi2212 single crystal was aligned within the a-b plane. To obtain the field dependence of the ZFC or FC magnetization at 4K, the sample was cooled down to 4K from above T_c at the field indicated at the corresponding hysteresis loop, of 0 Kgauss, 5 Kgauss and 10 Kgauss. Then the field was set to zero and the magnetization measured with increasing field up to 50 Kgauss, then in decreasing field down to -50 Kgauss and again up to the highest field to close the hysteresis loop. The magnetization results are shown in **Figs. 18** a and b. Indeed, as expected, no magnetization is observed at zero magnetic field when a zero magnetic field is applied. In contrast, a certain magnetization is observed at zero magnetic field when the sample is field cooled at 5 Kgauss. An even larger magnetization occurs at a cooling field of 10 Kgauss. A magnetization ratio of about 2 is obtained from Figs. 18 at H=0 in these field cooling processes of 5 Kgauss and 10 Kgauss, as expected.

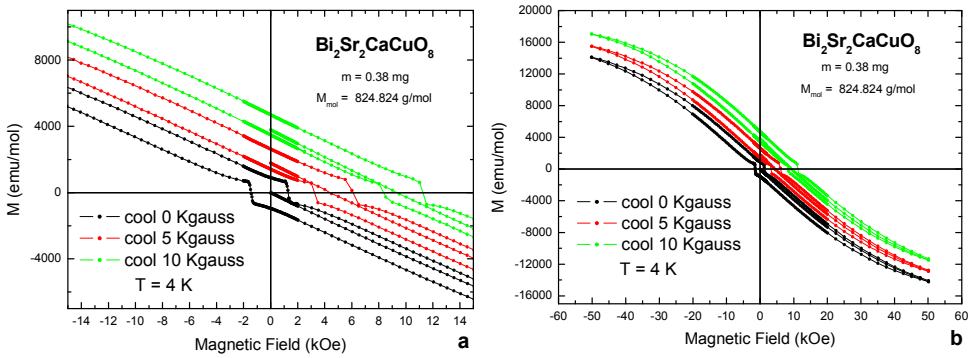

Figs. 18a and 18b. Magnetization as function of magnetic field in a Bi2212 crystal, field cooled at DC fields of 0, 5 and 10 Kgauss. Note that non zero magnetization is observed at zero magnetic fields when the compound is field cooled at 5 Kgauss or 10 Kgauss. It indicates the formation of JV remnant magnetization.

The memory results presented so far, did not involve the effect of temperature or time on the microwave-dissipaton signals. A limited experimental data related to time effects was achived as follows. After obtaining a H_m memory signal, the magnetic field was decreased to zero and kept at this field for 2 hours. Then the field was increased to a value above H_m to disclose the memory signal. The observed signal intensity and signal shape were similar to those observed earlier. It indicates that, if a time effect is present, it should be much longer than two hours.

The dependence of the maximum signal amplitude of a memory signal on the temperature was obtained as follows: A Bi2212 crystal aligned parallel to the a-b plane is cooled in a H_m field to 4K. After decreasing the field to zero, it was increased to a field that yields the maximum memory signal. Keeping the field constant the signal amplitude is measured by increasing temperature from 4K to 30K. The result is shown in Fig. 19. The figure illustrates that the amplitude of the memory signal remains constant in the temperature range 4K to 10K and decreases at higher temperature. This indicates that the JV remain frozen up to 10K and loose the equilibrium state with increasing temperature.

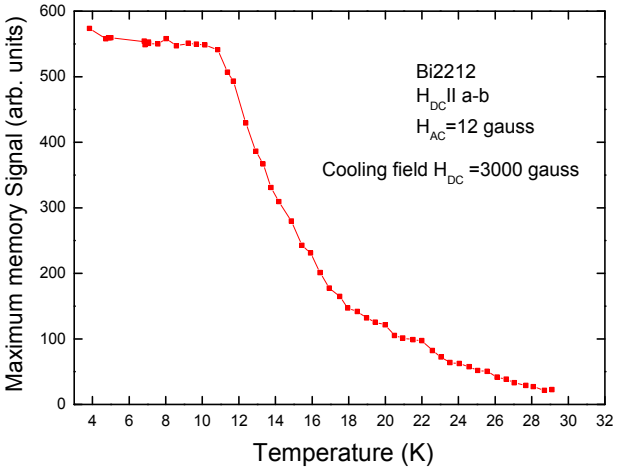

Fig. 19. Dependence of the maximum memory signal ampitude on temperature, derived from the memory signal after field cooling the sample to 4K and measuring the signal ampitude at the DC field of maxium memory signal on increasing the temperature continuously to higher values.

4.4 JV phase diagram

The magnetic field of the JV phase diagram, as function of temperature, derived from the results of the memory effect, is shown in Fig. 20. It indicates the presence of a glass state at the lowest temperature followed by a cross over state, an Anderson glass state, and a liquid state at higher temperatures.

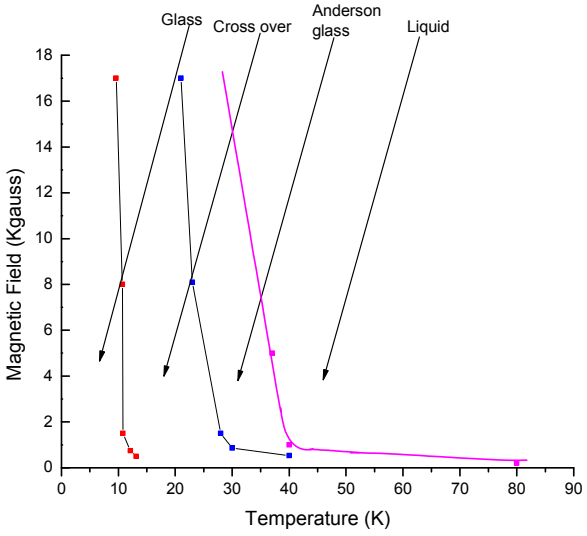

Fig. 20. Magnetic field-temperature phase diagram of JV in Bi2212.

4.5 Evaluating the possibility to study small or nano-scale superconducting systems with EPR spectrometers

The microwave-dissipation signal of a high T_c Bi2212 superconductor, shown in Fig. 21, is obtained from Fig. 2. The sample size was 10x10x0.1 mm^3. Its maximum intensity is of the order of 10,000 arbitrary units. The remarkably high intensity signal promises the possibility to investigate nano-scale superconductors and sizable small samples obtained by reducing the sample thickness to a few superconducting layers.

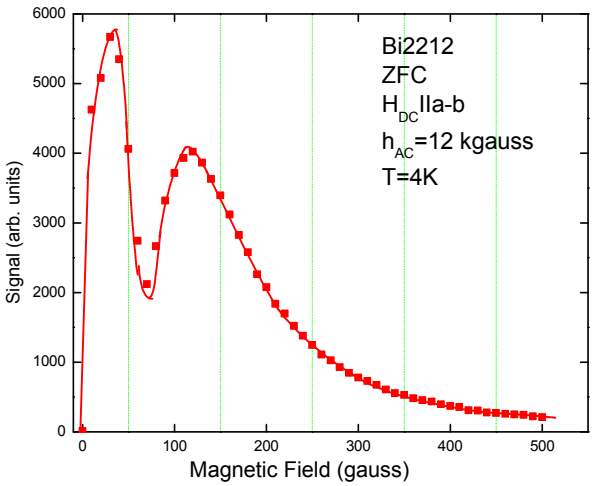

Fig. 21. Signal amplitude as function of magnetic field in a 10x10x0.1mm^3 Bi2212 crystal. The remarkable high intensity signal promises investigation of EPR properties in nano crystals.

Extremely thin superconductors with a limited number of layers are required when studying sample size effects on their properties. EPR technique can be considered in investigating their properties, by comparing results obtained in small layered nano crystals of similar structure with those obtained in crystals with a larger layer number. In samples with a small number of conducting layers the following EPR measurements are anticipated: a) Differences in the interaction between JV and AV vortices due to the small number of neighboring conducting layers. b) Results presented so far have shown that the observed properties depend on sample treatments, such as field cooling or zero field cooling procedure. Therefore the effect of cooling on thin samples may show different response that would depend on the sample thickness. c) The magnetic field memory effect, being by itself a very interesting effect, is explained using the hierarchical model of glassy state, commonly used in spin glass theory (Shaltiel et al., 2010). As the glassy state may depend on the thickness of the sample, it would be interesting to investigate the memory effect in small layer samples. Nano superconducting samples needed to investigate their properties are readily obtained using cleavage methods. In contrast the preparation method of thin superconductors for investigating IJJ properties, when regular methods are applied, is cumbersome, the reason being that conducting elements should be installed on the mesas' surface. Here we quote such a sample preparation in mesas that has been used to study teraherz-wave emission from Intrinsic Josephson Junctions in high T_c superconductors (Kadowaki et al., 2008): "The experiments were performed with the conventional methods commonly used in performing similar measurements and include

soldering of conducting wires on the sample's surface. Preparation of the mesas needs skilful techniques as can be deduced from the following description. "The samples were prepared from a piece of single crystal grown by the traveling floating zone method. A cleaved thin single crystal with a thickness of several μm was glued on a sapphire substrate by U-vanish (polyamide resin), and a silver thin layer and a gold film are sputtered on the cleaved sample surface. Then, the sample mesa and two contact pads with a desired size were patterned by the photolithography and Argon ion milling techniques. After removing unnecessary resist, CaF_2 is evaporated on the part of mesa for the electrical isolation purpose, and Au is finally deposited for the contact pad. This Au is again patterned by photolithography and Argon milling techniques again." In contrast to this difficult and cumbersome sample-preparation method in preparing thin mesas, preparation of samples to be used in investigating nano samples with the EPR technique can be described as follows: "A cleaved thin single crystal of conventional size should be glued on a sapphire with proper dimensions to fit the sample holder of the spectrometer". The contrast between the extremely complicated preparation method, where the so called "conventional measurement method" is used, and the simplicity in sample preparation in performing EPR nano measurements is striking. The EPR method should therefore be preferred in studying nano superconductors, when similar properties are to be investigated. Microwave emission from Intrinsic Josephson Junctions in high T_c superconductors can readily be investigated using a device where an AC modulating technique is applied, and whose features are similar to those of the EPR spectrometer. With such a device the microwave output will be modulated at AC frequency.

4.6 Searching for superconducting compounds, with EPR spectrometers

Fig. 22**,** derived from Fig. 1 of Shaltiel et al., 1991, plots, in schematic representation, the resistivity R(T,H) in cooling a superconductor from above to below T_c at different DC magnetic fields. The figure shows that an ESR signal is obtained when sweeping the temperature from above to below T_c. The signal is induced by the AC field. It results from variations of the sample resistivity during the cooling process that affects the quality factor Q of the cavity of the spectrometer. Thus, EPR spectrometers can be used to search for superconducting materials, to determine their T_c, to study resistivity in superconductors, and to investigate the effects of various paramenets on the sample resistivity, without applying wiring contacts.

4.7 Determination of the anisotropy in superconductors

A description of a procedure that measures the anisotropy in superconductors using an EPR spectrometer was reported earlier (Shaltiel et al., 1992)**.** The anisotropy was derived by analyzing EPR results of the signal-peak intensity, obtained when varying the temperature across T_c, as function of the orientation-angle θ of the magnetic field with respect to the crystal axis (Shaltiel et al., 1992)**.** The detailed description of the measuring procedure including analysis of the results is presented in the above article**.** The results derived from these measurements, agree with a theory proposed by Tinkham, where the superconducting anisotropy constant ε is involved. Values of ε = 5 and ε= 40-60 were obtained for YBCO and Bi2212, respectively (Shaltiel et al., 1992). The results described in Shaltiel et al., 1992, which show the dependence of the signal intensity as function of the orientation angle, are a guide that can be used to orient a superconducting crystal with respect to an externally applied magnetic field. The orientation of the superconducting crystal through all the measurements presented in this work were performed by this procedure.

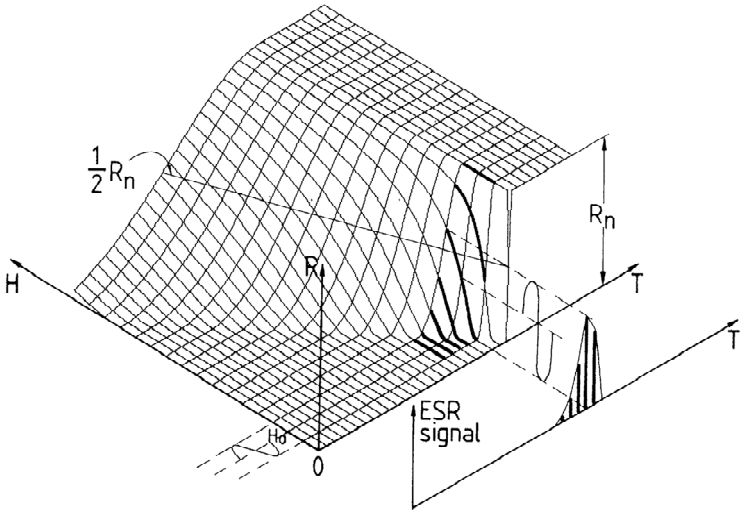

Fig. 22. Schematic, three dimensional presentation of the resistivity as function of magnetic field and temperature in a superconductor. Application of an AC field induces variation in the resistivity. The figure shows that an EPR signal is observed at the superconducting transition temperature.

5. Conclusion

The title of the present article: "Investigating the superconductivity with EPR (Electron Paramagnetic Resonance) spectrometer", also known as ESR (Electron Spin Resonance) spectrometer, is to a certain sense misleading but was intentionally chosen to put attention to an unconventional possibility to use the EPR technique. It gives the impression that the spectrometer investigates properties related to paramagnetic states and transitions between spin states in superconductors. As spin states and paramagnetic properties have not been an important subject in investigating properties in superconductors, various physicists ignore publications related to EPR technique. However, studying superconductors with EPR spectrometers generates a rich spectrum of experimental results of different nature. Hence, questions appeared regarding the mechanism that gives rise to the EPR signals and what do the results indicate. The present work provides answers to both questions. Investigating mesas shows that applying current in Josephson transmission lines (JTLs) induces motion of the fluxons that reside between the conduction planes and that the fluxons interact with the environment (Ustinov, 1998). Fig. 12 shows that in the case of EPR technique the AC modulation field induces Eddy currents that apply a Lorentz force that induces the motion of fluxons in the high anisotropy superconductors Bi2212 and Bi2223. Their motion interacts with the microwaves and induces the observed signal. This is the mechanism that provides the experimental results. The detailed theoretical derivation in the framework of Josephson phase electrodynamics (Shaltiel et al., 2008) enables to model the observed dependence of the microwave absorption on the DC magnetic field and the strong increase of the signal with increasing anisotropy. The analysis of the results yields information related to the properties of Josephson vortices in high anisotropy superconductors, which are otherwise not or only difficult to access. Here we recall two prominent achievements: (a) by means of

field cooling and zero-field cooling experiments a memory effect was discovered and a corresponding phase diagram of the Josephson-vortex system was derived. (b) From angular dependent measurements pinning of the Josephson vortices by Abricosov vortices was established. Hence, the EPR spectrometer is the experimental device that measures these properties. We note that it was originally designed to investigate different properties than those probed presently. Experimentally the spectrometer investigates properties of superconductors, where Josephson transmission lines are present. If such an instrument did not exist, it would have to be designed to enable the investigation of such properties.

6. References

Hechtfischer, G.; Kleiner, R.; Schlenga, K.; Walkenhorst, W. & Müller, P. (1997). Collective Motion of Josephson Vortices in Intrinsic Josephson Junctions in $Bi_2Sr_2CaCu_2O_{8+y}$. *Physical Review B*, Vol.55, No.21, (June 1997), pp. 14638-14644.

Kadowaki, K.; Yamaguchi, H.; Kawamata, K.; Yamamoto, T.; Minami, H.; Kakeya, I.; Welp, U.; Ozyuzer, L.; Koshelev, A.; Kurter, C.; Gray, K.E. & Kwok, W.-K. (2008). Direct Observation of Tetrahertz Electromagnetic Waves Emitted from Intrinsic Josephson Junctions in Single Crystalline $Bi_2Sr_2CaCu_2O_{8+\delta}$. *Physica C*, Vol.468, (April 2008), pp. 634-639.

Shaltiel, D.; Bill, H.; Grayevsky, A.; Junod, A.; Lovy, D.; Sadowski, W. & Walker, E. (1991). Microwave Absorption across T_c: Determination of the Angular Dependence $H_{c2}(\theta)/H_{c2}$. *Physical Review B*, Vol.43, No.16, (June 1991), pp. 13594-13597.

Shaltiel, D.; Ginodman, V.; Golosovsky, M.; Katz, U.; Boasson, H.; Gerhouser, W. & Fischer, P. (1992). Investigation of the Magnetic Field-induced Microwave Absorption across T_c in Single Crystals of $YBa_2Cu_3O_{7-\delta}$ and BiSrCaCuO Anisotropy and Magnetic Field Dependence. *Physica C*, Vol.202, (November 1992), pp. 303-320.

Shaltiel, D.; Bezalel, M.; Revaz, B.; Walker, E.; Tamegai, T. & Ooi, S. (2001). Dynamic Response of Microwave Absorption Triggered by Magnetic Modulation in High Anisotropy $Bi_2Sr_2CaCu_2O_x$ Crystals. *Physica C*, Vol.349, (January 2001), pp. 139-149.

Shaltiel, D.; Krug von Nidda, H.-A.; Loidl, A.; Rosenstein, B.; Shapiro, B.Ya.; Shapiro, I.; Tamegai, T. & Bogoslavsky, B. (2008). Sharp Increase of Microwave Absorption Due to Shaking of Josephson Vortices in BiSCCO Superconductor. *Physical Review B*, Vol.77, (January 2008), pp. 014508-1-014508-7.

Shaltiel, D.; Krug von Nidda, H.-A.; Shapiro, B. Ya.; Rosenstein, B.; Loidl, A.; Bogoslavsky, B.; Shapiro, I. & Tamegai, T. (2008a) Interaction between Josephson and pancake vortices investigated by the induced microwave dissipation by ac magnetic field technique, *Phys. Rev. B* 77, (June 2008), pp. 214522-1-214522-5.

Shaltiel, D.; Krug von Nidda, H.-A.; Rosenstein, B.; Shapiro, B.Ya.; Golosovsky, M.; Shapiro, I.; Loidl, A.; Bogoslavsky, B.; Fujii, T.; Watanabe, T. & Tamegai, T. (2010). Field Cooling Memory Effect in Bi2212 and Bi2223 Single Crystals. *Superconductor Science and Technology*, Vol.23, No.7, (July 2010), pp. 75001-75006.

Srinivasu, V.V.; Ken-ichi, I.; Hashizume, A.; Sreedevi, V.; Kohmoto, H.; Endo, T.; da Silva, R.R.; Kopelevich, Y.; Moehlecke, S.; Masui, T. & Hayashi, K. (2001). Nonresonant Microwave Absorption in Bi2212 Single Crystal: Second Peak and Microwave Power Dependence. *Journal of Superconductivity: Incorporating Novel Magnetism*, Vol.14, No.1,(February 2001), pp. 41-46.

Ustinov, A.V. (1998). Solitons in Josephson Junctions. *Physica D*, Vol.123, (November 1998), pp. 315-329.

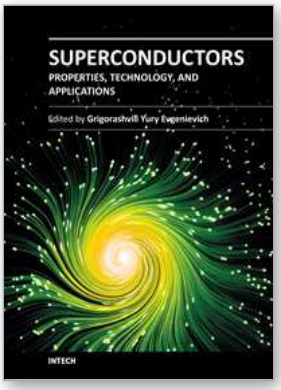

Superconductors - Properties, Technology, and Applications
Edited by Dr. Yury Grigorashvili

ISBN 978-953-51-0545-9
Hard cover, 436 pages
Publisher InTech
Published online 20, April, 2012
Published in print edition April, 2012

Book "Superconductors - Properties, Technology, and Applications" gives an overview of major problems encountered in this field of study. Most of the material presented in this book is the result of authors' own research that has been carried out over a long period of time. A number of chapters thoroughly describe the fundamental electrical and structural properties of the superconductors as well as the methods researching those properties. The sourcebook comprehensively covers the advanced techniques and concepts of superconductivity. It's intended for a wide range of readers.

How to reference
In order to correctly reference this scholarly work, feel free to copy and paste the following:

D. Shaltiel, H.A. Krug von Nidda, B.Ya. Shapiro, A. Loidl, T. Tamegai, T. Kurz, B. Bogoslavsky, B. Rosenstein and I. Shapiro (2012). Investigating Superconductivity with Electron Paramagnetic Resonance (EPR) Spectrometer, Superconductors - Properties, Technology, and Applications, Dr. Yury Grigorashvili (Ed.), ISBN: 978-953-51-0545-9, InTech, Available from: http://www.intechopen.com/books/superconductors-properties-technology-and-applications/investigating-superconductivity-with-electron-paramagnetic-resonance-epr-spectrometer

INTECH
open science | open minds

InTech Europe
University Campus STeP Ri
Slavka Krautzeka 83/A
51000 Rijeka, Croatia
Phone: +385 (51) 770 447
Fax: +385 (51) 686 166
www.intechopen.com

InTech China
Unit 405, Office Block, Hotel Equatorial Shanghai
No.65, Yan An Road (West), Shanghai, 200040, China
中国上海市延安西路65号上海国际贵都大饭店办公楼405单元
Phone: +86-21-62489820
Fax: +86-21-62489821

© 2012 The Author(s). Licensee IntechOpen. This is an open access article distributed under the terms of the Creative Commons Attribution 3.0 License, which permits unrestricted use, distribution, and reproduction in any medium, provided the original work is properly cited.